Article

High-Performance Microcrystalline Cellulose/Soy Protein Isolate-Based Nanocomposite Film via Cu and Zn Nanoclusters Modification

Kuang Li [1,2], Shicun Jin [1,2], Hui Chen [1,2,*], Jing He [1,2,*], Jianzhang Li [1,2,*]

[1] Key Laboratory of Wood Material Science and Utilization, Beijing Forestry University, Beijing 100083, China; kuangli@bjfu.edu.cn (K.L.); jinsc1994@bjfu.edu.cn (S.J.)

[2] Ministry of Education, Beijing Key Laboratory of Wood Science and Engineering, College of Materials Science and Technology, Beijing Forestry University, 35 Tsinghua East Road Haidian District, Beijing, 100083, China

* Correspondence: chenhui@bjfu.edu.cn (H.C.); Hejing2008@sina.com (J.H.); lijzh@bjfu.edu.cn (J.L.); Tel.: +86-010-62336912 (H.C.)

Abstract: Soy protein isolate (SPI) based materials are abundant, biocompatible, renewable, and biodegradable. In order to improve the tensile strength (TS) of SPI films, we prepared a novel composite film modified with microcrystalline cellulose (MCC) and metal nanoclusters (NCs) in this research. The effects of the modification of MCC on the properties of SPI-Cu NCs and Zn NCs films were investigated. Attenuated total reflectance-Fourier transformed infrared spectroscopy analyses and X-ray diffraction patterns characterized the strong interactions and reduction of the crystalline structure of the composite films. Scanning electron microscope showed the enhanced cross-linked and entangled structure of modified films. Compared with untreated SPI film, the tensile strength of the SPI-MCC-Cu and SPI-MCC-Zn films increased from 2.91 MPa to 13.95 and 6.52 MPa, respectively. Moreover, the results also indicated their favorable water resistance with higher water contact angle. Meanwhile, the composite films exhibited increased initial degradation temperatures, demonstrating their higher thermostability. The results suggested that MCC could effectively improve the performance of SPI-NCs films, which would provide a novel preparation method for environmentally friendly SPI-based films in the applications of packaging materials.

Keywords: soy protein isolate; microcrystalline cellulose; metal nanoclusters; nanocomposite film; tensile strength

1. Introduction

Driven by the environmental problems caused by using petroleum-derived polymers, the requirement of the development of eco-friendly materials for agriculture, packaging, and coating industries has greatly increased [1]. Due to renewability and biodegradability, biopolymer materials made from natural resources such as proteins, cellulose, and polysaccharides are regarded as an attractive alternative to the development of environment friendly materials [2]. It is reported that nanoparticles had an effect on protein-based films, but the tensile strength was still relatively poor [3]. In order to further improve the mechanical property of protein film, we prepared a novel nanocomposite film modified with microcrystalline cellulose (MCC).

Compared with other proteins, soy protein has been extensively investigated for the development of biodegradable films due to its abundance, low cost, biodegradability, and biocompatibility [4,5]. Soy protein isolate (SPI) is a mixture of proteins containing approximately 90% globulins. 7S and 11S, which amount about 37% and 31% of major globulins of SPI, have good film-forming ability and polymerization [6,7]. However, relative low strength and poor water resistance have become the main drawbacks of natural SPI-based products and limit their further applications. Therefore, efforts should be made to modify their properties for commercial application.

In recent years, growing interest has been devoted to materials derived from functional nanomaterials mainly due to its great potential for applications in the fields of biology, biomedicine, energy conversion, catalysis and chemical sensors [8]. Metal nanoclusters (NCs, < 2 nm), emerging as a novel functional nanomaterials, are defined as isolated particles composed of a few to hundreds atoms [9]. The dimension of this particle approaches the Fermi wavelength of electrons. Their discrete energy levels of electrons make their optical, electronic and chemical properties markedly different from conventional bulk materials [10]. Due to its reduced size, this particle exhibits even higher surface-to-volume ratios than conventional nanoparticles [11]. Most importantly, reports have revealed that metal NCs could have an obvious effect on the physicochemical properties and subsequent biological responses of natural polymers [12]. Particularly, among other noble metals, Cu NCs and Zn NCs exhibited significant advantages such as relative high biocompatibility, water solubility, and excellent stability, which make them attract considerable interest and have more possibilities for potential applications in various areas [13]. In our previous research, we prepared SPI-based film modified with Cu NCs and Zn NCs. However, these films also exhibited some drawback such as relatively low mechanical and hydrophobic properties. Therefore, further researches about modification of SPI-NCs films are still needed to be done.

As the most abundant biopolymer in nature, cellulose has been used widely in the textiles, agriculture, and food industry [14,15]. Microcrystalline cellulose (MCC) is cellulose derivative obtained from acid hydrolysis of wood fiber, back neutralization with alkali and spray dried [16,17]. It is an anionic biopolymer with relatively high cellulose content and crystallinity, the reinforcing phase has both a high aspect ratio and bending strength in synthetic composites [18]. Due to its renewable nature, large specific surface area, and unique physicochemical properties, MCC has great promising applications in biocomposites, protein immobilization, drug delivery, and metallic reaction template [19]. Recently, the modification of MCC in polymer composites has been a subject of intense research, such as protein, chitosan, wheat bran, and corn starch [20-22]. Unfortunately, MCC/SPI composite films still exhibit relatively poor performances in mechanical and permeability properties, which need further research.

In this study, in order to further improve the tensile strength, water resistance ability, and thermal stabilities of SPI-based films modified with Cu NCs and Zn NCs, we modified this nanocomposite film with microcrystalline cellulose (MCC). The effects of the modification of MCC on the properties of SPI-NCs films were investigated. These composite films were characterized by Fourier transform infrared spectroscopy (FTIR), X-ray diffraction (XRD), and scanning electron microscope (SEM). Mechanical properties, water resistance ability, and thermal stabilities were also investigated. The effects of these functional properties might have a great importance in the applicability of SPI-based films as renewable and biodegradable packaging materials.

2. Materials and Methods

2.1 Materials

SPI with 95% protein content was provided by Yuwang Ecological Food Industry Co., Ltd. Microcrystalline cellulose (MCC, $(C_6H_{10}O_5)_n$) was provided by Sinopharm Chemical Reagent Co., Ltd. Copper sulphate anhydrous and zinc chloride purchased from Beijing Chemical Works were used to prepare Cu NCs and Zn NCs solution. Glycerol with 99% purity and sodium hydroxide of analytical grade were purchased from Beijing Chemical Reagents. All solutions were prepared with deionized water.

2.2 Fabrication of SPI-Cu NCs and SPI-Zn NCs

4.0 g SPI was dispersed in 80 mL distilled water with a magnetic stirrer to prepare SPI solutions. Then, 8 mL $CuSO_4$ or $ZnCl_2$ (20 mmol/L) was dispersed in these SPI solution. The mixture was adjust pH about 12 with NaOH solution and constantly stirred at 25 °C for 10 min. The mixed solution was heated with a magnetic stirrer at 75 °C for 8 h to prepare Cu NCs and Zn NCs.

2.3 Preparation of SPI/MCC nanocomposite films

The SPI/MCC films were prepared by casting method. 2.0 g glycerol (50% of SPI, w/w) and 1.6 g MCC (40% of SPI, w/w) were dispersed in these SPI-Cu NCs or SPI-Zn NCs solutions prepared before. The mixed solutions were heated with a water bath at a temperature of 85 °C for 30 min. Then, the solutions were subsequently poured into leveled Teflon plates and cast with the same amount (40 g). Films were dried in a vacuum drying oven at 45 °C for 24 h and placed in a controlled chamber under the condition of 25 °C and 50% relative humidity for a week before testing.

2.4. Characterization of SPI/MCC nanocomposite films

2.4.1. High resolution transmission electron microscopy (HRTEM)

HRTEM images of SPI-Cu NCs and SPI-Zn NCs were performed on FEI Tecnai G2F20 transmission electron microscopy at 200 kV of acceleration voltage (FEI, Oregon, USA).

2.4.2. Attenuated Total Reflectance-Fourier Transform Infrared Spectroscopy

Structural characteristics of SPI-based films were investigated with attenuated total reflectance-Fourier transformed infrared (ATR-FTIR) spectra on a spectrometer (Nicolet 6700), the scan width was 4000-650 cm^{-1} through 32 scans.

2.4.3. X-Ray Diffraction Analysis

X-ray diffraction (XRD) was carried out to investigate structural changes of the different films on a D8 Advance diffractrometer (Bruker AXS, Germany) with a Cu-Kα radiation source in continuous scanning mode. The samples were scanned with a range from 5° to 60° and a step interval of 0.02° at a voltage of 45 kV.

2.4.4. Scanning Electron Microscope

Scanning electron microscope (SU8010, Hitachi) was carried out to characterize the cross-section morphologies of the specimens with an acceleration voltage of 5 kV.

2.4.5. Mechanical Properties

Tensile properties were examined using tensile testing machine (DCP-KZ300) at a speed of 20 mm/min at 25 °C and 50% relative humidity. The initial gauge length of each samples was 50 mm. The average values of tensile strength (TS), elongation at break (EB) and Young's modulus (E) was calculated with five specimens (80 mm × 10 mm^2).

2.4.6. Thermogravimetric Analysis

The Q50 TGA analyzer (TA Instrument, USA) was carried out to investigate the thermal stability of SPI-based films. Each sample was dried at 105 °C for 24 h in a air-circulating oven before testing. Film specimens were scanned from 25 °C to 600 °C at a heating rate of 10 °C/min under nitrogen atmosphere (100 mL/min).

2.4.7. Contact Angles Determination

The surface hydrophobicity of each film was measured by water contact angle with a contact angle meter (OCA20, Dataphysics Co., Ltd, Germany). A film sample (20 × 80 mm^2) was placed on a movable carrier and leveled horizontally. Each sessile droplet of distilled water was controlled at 3 μL and dropped onto the surface of films. Five replicates were measured for each film.

2.4.8. Water Resistance

Five samples of each film were conducted to determine their moisture content. Film specimens were weighted at room temperature and marked as initial mass (m_0). Then, the samples were dried in an air-circulating oven at a temperature of 105 °C for 24 h and then weighted again (m_1). Moisture content (MC) of each sample was calculated as follows:

$$MC\ (\%) = (m_0 - m_1)/m_0 \times 100 \quad (1)$$

Afterwards, samples were submerged in a covered bottle with distilled water (30 mL) at 25°C for 24 h. Then, the samples were dried in an air-circulating oven at a temperature of 105 °C for 24 h and weighted (m_2). Total soluble matter (TSM) was calculated as follows:

$$TSM\ (\%) = (m_1 - m_2)/m_1 \times 100 \quad (2)$$

The water absorption of specimens were measured in a desiccator with P_2O_5 desiccant at 0% relative humidity for 48 h and initial weight was recorded as m_3. Then, the specimens were immersed in a covered bottle with 30 mL of distilled water at room temperature for 24 h. The water on the surface of sample was removed and then weighed again (m_4). Water absorption (WA) was calculated as follows:

$$WA\ (\%) = (m_4 - m_3)/m_3 \times 100 \quad (3)$$

3. Results

3.1. Characterization of SPI-based Cu NCs and Zn NCs.

High resolution transmission electron microscopy (HRTEM) images were carried out to characterize the morphology of Cu NCs and Zn NCs. As shown in Figure 1, new substance of Cu NCs and Zn NCs had been formed successfully. Cu NCs were uniform, discrete and spherical particles with an average diameter about 5 nm. The so small size of particles indicated that Cu NCs consisted of a few metal Cu atoms. Meanwhile, Zn NCs were also observed in the prepared solution with a average size less than 10 nm.

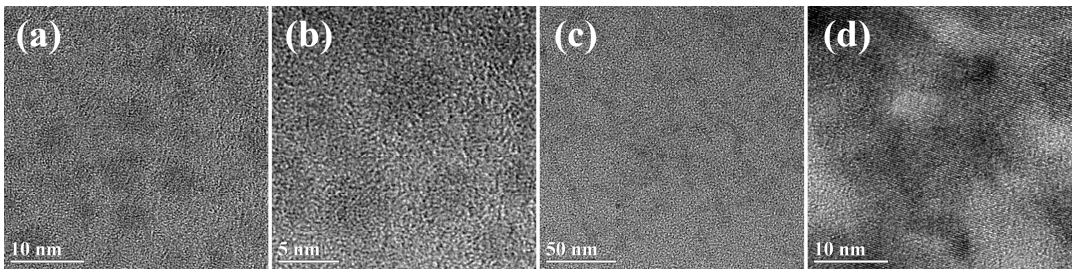

Figure 1. HRTEM images of Cu NCs (a and b) and Zn NCs (c and d) capped with soy protein isolate.

3.2. Structural analysis

In order to study the effects of MCC and metal NCs on structural characteristics of the SPI films, Attenuated Total Reflectance-Fourier Transform Infrared (ATR-FTIR) spectroscopy analyses (Figure 2a) were conducted. The bands at about 3500-3000 cm^{-1} were related to the free and associate O-H and N-H bending vibrations, which could form hydrogen bonding with the carbonyl groups of the peptide linkage of the protein [23]. The absorption bands at 2930 and 2875 cm^{-1} were related to the C-H stretching bands of CH2 and CH3 groups, and C-H bending band was observed at 1449 cm^{-1} [24]. The peak at 1038 cm^{-1} belongs to C-O stretching. The characteristic amide bands of soy proteins at 1628, 1536, and 1234 cm^{-1} were assigned to amide I (C-O stretching), amide II (N-H bending) and amide III (C-H and N-H stretching), respectively [25]. These featured bands were reported that might be affected by hydration and protein-solvent interactions [26]. With the addition of MCC, amide I and II of SPI-MCC film shifted to 1626 and 1537 cm^{-1}, respectively, indicating the films might expose

more polar groups and increase the bindings between the peptide chains [27]. Meanwhile, it was observed that composite films modified with MCC exhibited a new peak at 1160 cm^{-1}, which was attributed to the bending mode of C-CH_2-C, suggesting the unique bands of cellulose [28]. These results demonstrated that molecular hydrogen bonding might be formed between protein molecule chains and polar groups with the modification of MCC, which resulting in a cross-linked structure and improving mechanical properties of the composite films [29].

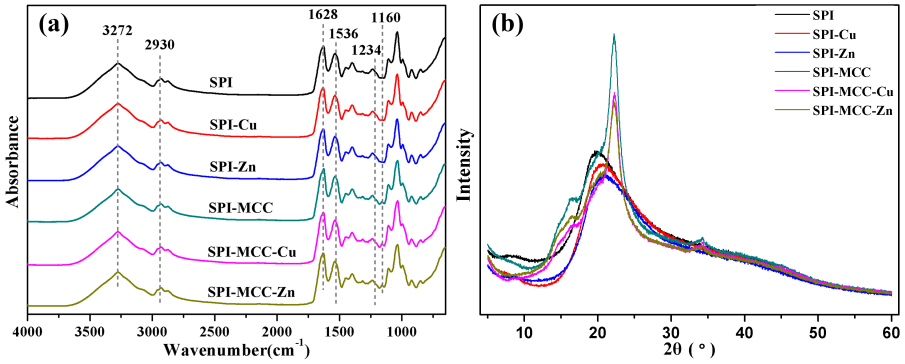

Figure 2. (a) ATR-FTIR spectra of untreated SPI films and SPI films modified with Cu NCs, Zn NCs, and MCC; (b) X-ray diffraction patterns of untreated SPI films and SPI films modified with Cu NCs, Zn NCs, and MCC.

X-ray diffraction (XRD) patterns of composite films were shown in Figure 2b. The MCC powder exhibited four characteristic crystalline peaks around 2θ = 14.8°, 16.2°, 22.6° and 34.5°, corresponding to (-1 1 0), (1 1 0), (2 0 0) and (4 0 0) lattice planes respectively, which was a characteristic of cellulose I structure [30]. It was reported that the parallel chains in this crystals were strongly inter-molecularly hydrogen bonded [31].

Control film showed a strong characteristic peak of SPI at 2θ values of around 20.0° and SPI-MCC films had strong characteristic peaks of MCC around 2θ = 14.8°, 16.2°, 22.6° and 34.5°. The films modified with MCC exhibited relatively high peaks, indicating that MCC had a high crystalline structure and thus increased the rigid of the films. Compared with SPI and SPI-MCC film, the intensity of these peaks of the films modified with metal NCs were greatly decreased, which was probably caused by the reason that the original crystalline structure of MCC had been partially destroyed during the interactions with SPI [32]. The crystalline structure had collapsed and exposed more active groups and prompted more reactions, which resulted in the reduction of the crystalline structure of the modified films [33].

3.3. Micromorphology

The cross-section morphology of the films was observed by scanning electron microscope (SEM) micrographs. As seen in Figure 3a, the SPI film without modification exhibited a relatively smooth and continuous surface, indicating there were less physical interactions in SPI films. The images (Figure 3b) showed that the cross-sections of SPI-Cu NCs film was more homogeneous and smoother, it indicated Cu NCs were well dispersed in the SPI matrix. From Figure 3c, the SPI-Zn film showed a relatively coarse and regular surface, which revealed the good compatibility and uniform distribution of SPI and Zn NCs. However, with the addition of MCC, the films became rather coarse and fluctuant, the presence of cracks and scratches were also observed in the fracture surface (Figure 3d-f), demonstrating the entanglement and strong interactions between SPI and MCC, thereby resulting in the characteristic of tough fracture and a cross-linked structural formation in the film [34]. These findings confirmed that MCC had a great influence on the structure of the SPI-NCs films, thus enhanced mechanical properties discussed above.

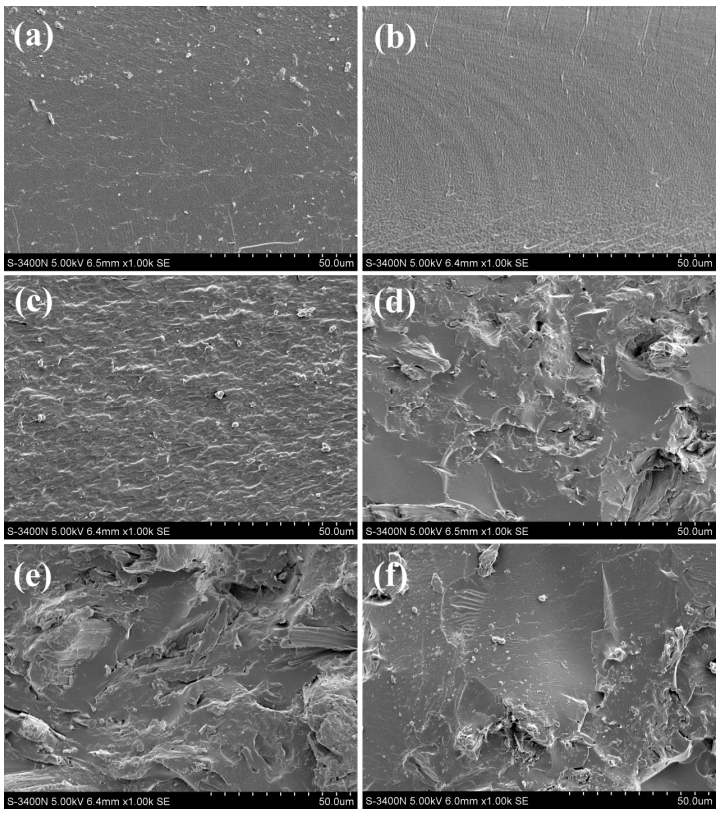

Figure 3. SEM micrographs of the fracture surface of SPI-based films: (a) SPI film; (b) SPI-Cu film; (c) SPI-Zn film; (d) SPI-MCC film; (e) SPI-MCC-Cu film; and (f) SPI-MCC-Zn film.

3.4. Physical and mechanical properties

The tests results of mechanical properties of experimental films were showed in Table 1. Generally, films formed from purely soy protein isolate tend to be brittle, thus the SPI film exhibited relative low mechanical properties. The TS of SPI-Cu and SPI-Zn film were 4.78 and 4.56 MPa, which were probably due to an increase in the number of potential intermolecular interactions and lead to a higher degree of cross-linking in the nanocomposite films. Compared with untreated SPI film, the incorporation of MCC also increased the TS from 2.91 to 4.04 MPa, indicating higher strength of the films. This result was in accordance with those studies reported before [35]. Furthermore, the SPI-MCC-Cu films exhibited highest TS with the value of 13.95 MPa. The reason was related to the interfacial interaction between the composite matrix and NCs [36]. This fact was probably due to the MCC had an effect on increasing the number of potential intermolecular interactions and led to a higher degree of cross-linking in the nanocomposite film [37]. Not only plasticizing the protein matrix, the cellulose microfibrils might also interact more preferentially with the NCs, thereby enhanced the protein-fiber interfaces.

Table 1. Thickness, tensile strength (TS), elongation at break (EB), and Young's modulus (E) of untreated SPI films and SPI films modified with Cu NCs, Zn NCs, and MCC.

Films	Thickness(mm)	TS (MPa)	EB (%)	E(MPa)
SPI	0.158 (0.023) [a]	2.91 (0.27)	164.90 (0.07)	55.48 (3.62)
SPI-Cu	0.271 (0.015)	4.78 (0.30)	69.13 (0.03)	144.00 (3.35)
SPI-Zn	0.260 (0.017)	4.56 (0.16)	168.30 (0.12)	118.50 (2.14)
SPI-MCC	0.255 (0.027)	4.04 (0.40)	29.57 (0.07)	154.90 (2.31)
SPI-MCC-Cu	0.335 (0.019)	13.95 (0.09)	17.12 (0.15)	554.70 (4.64)

SPI-MCC-Zn	0.248 (0.020)	6.52 (0.30)	26.82 (0.10)	258.40 (3.73)

[a] Mean (standard deviation).

Flexibility was also an important mechanical property of the soy protein film which was reflected by the EB. Untreated SPI film exhibited a relatively high flexibility with EB of 164.90 %. After modified with NCs, the SPI-Zn film showed higher EB than that of SPI-Cu film, indicating that Zn NCs had better performance on the flexibility of the films. However, the EB of SPI films modified with MCC obviously decreased, it was might attribute to the heterogeneous combination of celluloses and protein, which decreased the composite film's interfacial stress transfer and caused stiffness [38].

3.5. Thermal stabilities

The property of thermal stabilities of the films was tested by thermal gravimetric (TG) and derivative thermal gravimetric (DTG), the results were illustrated in Figure 4 and Table 2. Thermal gravimetric curves of the films consisted of three stages (Figure 4a). The initial weight loss from 50 °C to 120 °C was attributed to the evaporation of residual moisture in SPI film, while the second stage from 120 °C to 270 °C was mainly assigned to the evaporation of glycerol, and the third stage from 270 °C to 450 °C was related to the backbone peptides degradation [39]. Particularly, the main weight loss stage at 350 °C was caused by the degradation of carbonaceous matter in MCC [40].

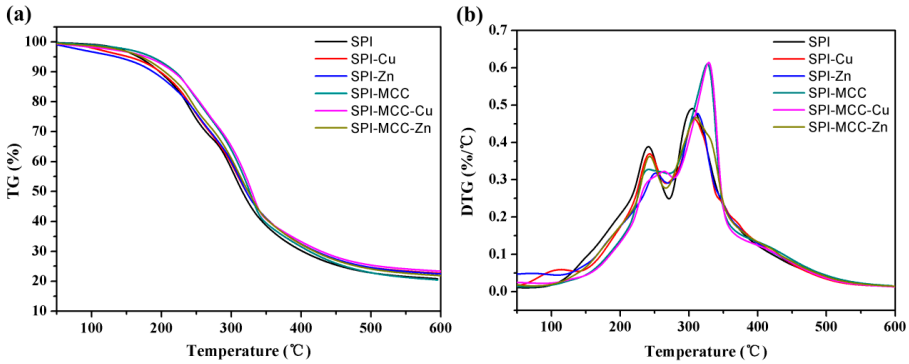

Figure 4. (a) Thermo gravimetric (TG) and (b) derivative thermo gravimetric (DTG) curves of untreated SPI films and SPI films modified with Cu NCs, Zn NCs, and MCC.

Table 2. Thermo-degradation data of untreated SPI films and SPI films modified with Cu NCs, Zn NCs, and MCC.

Films	T_{i1}(°C)	T_{max1}(°C)	T_{i2}(°C)	T_{max2}(°C)
SPI	146.72	239.98	286.55	304.85
SPI-Cu	155.83	241.63	291.94	308.17
SPI-Zn	178.68	251.38	295.28	312.84
SPI-MCC	168.42	235.85	304.94	328.39
SPI-MCC-Cu	183.59	243.26	309.54	329.06
SPI-MCC-Zn	170.44	243.28	305.16	310.81

T_i: Initial temperature of degradation; T_{max}: Temperature at maximum degradation rate.

As listed in Table 2, the initial degradation temperatures (T_{i2}) of SPI films modified with MCC were higher than that of other films, indicating the presence of abundant hydrogen bonds groups formed in the protein chains [41]. Moreover, SPI-MCC-Cu film had the maximum degradation rate (T_{max2}) at highest temperature in DTG curve, compared with control film, it increased from 304.85 °C to 329.06 °C obviously, which might be attributed to the cross-linking reactions among MCC, NCs and SPI. Therefore, we could draw a conclusion that the thermal stability of the SPI-NCs films was improved by the modification of MCC.

3.6. Water Resistance

Measuring the contact angle of water droplet on surfaces was an important method to investigate the hydrophobicity of film surfaces. Generally, a high contact angle indicated high hydrophobicity of the surface. As shown in Table 3, control film presented a contact angle of about 48.36°, corresponding to a relatively high hydrophilic surface. After modified with NCs, the SPI-Cu and SPI-Zn films exhibited contact angles of 34.54° and 51.49°, which demonstrating that Zn NCs had a better performance on the surface hydrophobicity of SPI film. With the addition of MCC, the water contact angle of SPI-MCC film reduced to 42.37°, indicating a decrease in the hydrophobicity of the films. Similar observations were previously reported for MCC films [42]. However, it was worth noting that SPI-MCC-Cu film represented an obviously increase in the contact angle with a value of 58.03°, which was highest among all films. This result suggested this composite film might expose more polar groups and hydrophobic amino acids to the surface, and thus improved the water resistance [43].

Table 3. Water Contact angles, moisture content (MC), total soluble matter (TSM), and water absorption (WA) of untreated SPI films and SPI films modified with Cu NCs, Zn NCs, and MCC.

Films	Contact angles (°)	MC (%)	TSM (%)	WA (%)
SPI	48.36 (1.8) [a]	15.80 (1.2)	36.79 (1.0)	197.32 (8.3)
SPI-Cu	34.54 (2.8)	15.44 (1.8)	38.99 (0.9)	210.21 (6.9)
SPI-Zn	51.49 (2.8)	15.49 (1.5)	36.91 (0.8)	200.06 (6.7)
SPI-MCC	42.37 (1.1)	13.40 (1.7)	29.63 (1.2)	119.86 (7.0)
SPI-MCC-Cu	58.03 (1.9)	11.68 (2.1)	10.13 (0.8)	94.86 (6.5)
SPI-MCC-Zn	47.11 (2.1)	13.96 (1.8)	27.36 (1.0)	162.88 (5.0)

[a] Mean (standard deviation).

The water resistance of SPI-based films could be characterized by moisture content (MC), which were considered as important properties from a packaging materials view. The amount of water present in films was determined by MC, which was shown in Table 3. The MC of unmodified SPI film was relatively high, and there was not obviously different between SPI and the films modified with metal NCs, indicating that the addition of NCs did not significantly affect the water resistance of the SPI films. However, the MC of SPI film decreased from 15.80 to 13.40% when MCC was incorporated, and the SPI-MCC-Cu film exhibited the lowest MC with the value of 11.68%. This could be justified by the fact that MCC and metal NCs brought significant barrier properties and there were some specific interactions among MCC, NCs and SPI that stabilize the film structure [44], which was consistent with the ATR-FTIR and XRD results.

Total soluble matter (TSM) and water absorption (WA)were also considered as the indicators of the films resistance to water. Generally, lower values would indicate better water resistance. Compared to the control film, the TSM and WA of the films modified with NCs were slightly increased. With the addition of MCC, both TSM and WA significantly decreased from 36.79% and 197% to 29.63% and 119%, respectively. Furthermore, the TSM and WA of SPI-MCC-Cu film were the lowest among other films that decreased to 94.86% and 10.13%, indicating the best water resistance of the composite film. The results confirmed that the molecules of MCC and NCs might greatly crosslink the polymeric network of SPI and decrease the swelling of soy protein matrix under high moisture [45,46]. Therefore, SPI-MCC-Cu films prevented the permeation of water molecules and exhibited lower TSM and WA values.

4. Conclusions

This study showed the preparation of plant-derived biodegradable materials through the casting methodology of SPI modified with MCC and NCs. FTIR showed that the hydrogen bonding and cross-linking interaction in the film. The efficiency the crystalline structures of the SPI films changed

by the MCC and NCs were evidenced by XRD patterns. The SPI-MCC-Cu film had the highest tensile strength increased from 2.91 to 13.95 MPa. The enhanced entanglement and cross-linking in the microstructure of the films were observed by SEM. The composite films modified with MCC exhibited higher contact angle and lower MC, TSM, WA values, which indicated their better water resistance. Compared to the unmodified SPI film, these composite films also exhibited better thermal stability. Among these tests, the mechanical properties of nanocomposite films modified with MCC were improved most obviously. Therefore, the use of these protein-based biodegradable materials with improved properties might provide a valuable opportunity to replace conventional petroleum-derived plastics and add more value to this vast agricultural resource as packing materials.

Acknowledgment: The authors are grateful for financial support from the Fundamental Research Funds for the Central Universities (BLX201601), the Beijing Natural Science Foundation (2151003) and the Special Fund for Forestry Research in the Public Interest (Project 201404501).

Author Contributions: Kuang Li and Hui Chen conceived the project and designed the experiments; Kuang Li and Shicun Jin performed the experiments and analysed the data; Kuang Li wrote the main manuscript text; Hui Chen, Jing He and Jianzhang Li supervised and directed the project; All authors reviewed the manuscript.

Conflicts of Interest: The authors declare no conflict of interest.

References

1. Kaewprachu, P.; Osako, K.; Benjakul, S.; Rawdkuen, S. Effect of protein concentrations on the properties of fish myofibrillar protein based film compared with PVC film. *J. Food. Sci. Tech.* **2016**, *53*, 2083-91.
2. Xu, F.; Dong, Y.; Zhang, W.; Zhang, S.; Li, L.; Li, J. Preparation of cross-linked soy protein isolate-based environmentally-friendly films enhanced by PTGE and PAM. *Ind. Crop. Prod.* **2015**, *67*, 373-380.
3. Li, K.; Chen, H.; Li, Y.; Li, J.; He, J. Endogenous Cu and Zn nanocluster-regulated soy protein isolate films: excellent hydrophobicity and flexibility. *RSC Adv.* **2015**, *5*, 66543-66548.
4. Lee, J.-H.; Yang, H.-J.; Lee, K.-Y.; Song, K. B. Preparation and application of a flaxseed meal protein film containing lemongrass (Cymbopogon citratus) oil. *Int. J. Food Sci. Tech.* **2016**, *51*, 1473-1480.
5. Pan, H.; Jiang, B.; Chen, J.; Jin, Z. Blend-modification of soy protein/lauric acid edible films using polysaccharides. *Food Chem.* **2014**, *151*, 1-6.
6. Ma, L.; Yang, Y.; Yao, J.; Shao, Z.; Chen, X., Robust soy protein films obtained by slight chemical modification of polypeptide chains. *Polym. Chem.* **2013**, *4*, 5425.
7. Kang, H.; Song, X.; Wang, Z.; Zhang, W.; Zhang, S.; Li, J., High-performance and fully renewable soy protein isolate-based film from microcrystalline cellulose via bio-inspired poly(dopamine) surface modification. *Acs Sustain. Chem. Eng.* **2016**, *4*, 4354-4360.
8. Coupry, D. E.; Butson, J.; Petkov, P. S.; Saunders, M.; O'Donnell, K.; Kim, H.; Buckley, C.; Addicoat, M.; Heine, T.; Szilagyi, P. A., Controlling embedment and surface chemistry of nanoclusters in metal-organic frameworks. *Chem. Commun.* **2016**, *52*, 5175-8.
9. Shang, L.; Nienhaus, G. U., Metal nanoclusters: Protein corona formation and implications for biological applications. *Int. J. Biochem. Cell. B.* **2016**, *75*, 175-9.
10. Tao, Y.; Li, M.; Ren, J.; Qu, X., Metal nanoclusters: novel probes for diagnostic and therapeutic applications. *Chem. Soc. Rev.* **2015**, *44*, 8636-63.
11. Jin, R., Atomically precise metal nanoclusters: stable sizes and optical properties. *Nanoscale* **2015**, *7*, 1549-65.
12. Wu, Z.; Liu, J.; Gao, Y.; Liu, H.; Li, T.; Zou, H.; Wang, Z.; Zhang, K.; Wang, Y.; Zhang, H.; Yang, B., assembly-induced enhancement of cu nanoclusters luminescence with mechanochromic property. *J. Am. Chem. Soc.* **2015**, *137*, 12906-13.
13. Chen, H.; Lin, L.; Li, H.; Li, J.; Lin, J.-M., Aggregation-Induced StructureTransition of Protein-Stabilized Zinc/Copper Nanoclusters for Amplified Chemiluminescence. *ACS Nano.* **2015**, *9*, 2173-2183.
14. Nguyen, H.-L.; Jo, Y.; Cha, M.; Cha, Y.; Yoon, D.; Sanandiya, N.; Prajatelistia, E.; Oh, D.; Hwang, D., Mussel-Inspired Anisotropic Nanocellulose and Silver Nanoparticle Composite with Improved Mechanical Properties, Electrical Conductivity and Antibacterial Activity. *Polym.* **2016**, *8*, 102.
15. Reddy, K. O.; Maheswari, C. U.; Shukla, M., Physico-Chemical Characterization of Cellulose Extracted from Ficus Leaves. *J. Biobased. Mater. Bio.* **2013**, *7*, 496-499.

16. Miao, C.; Hamad, W. Y., Cellulose reinforced polymer composites and nanocomposites: a critical review. *Cellulose.* **2013**, *20*, 2221-2262.
17. Xu, D.; Zhang, J.; Cao, Y.; Wang, J.; Xiao, J., Influence of microcrystalline cellulose on the microrheological property and freeze-thaw stability of soybean protein hydrolysate stabilized curcumin emulsion. *Lwt-Food Sci Technol.* **2016**, *66*, 590-597.
18. da Silva, J. R. T.; de O. Farias, E. A.; Filho, E. C. S.; Eiras, C., Development and characterization of composites based on polyaniline and modified microcrystalline cellulose with anhydride maleic as platforms for electrochemical trials. *Colloid. Polym. Sci.* **2014**, *293*, 1049-1058.
19. Vanhatalo, K.; Lundin, T.; Koskimäki, A.; Lillandt, M.; Dahl, O., Microcrystalline cellulose property–structure effects in high-pressure fluidization: microfibril characteristics. *J. Mater. Sci.* **2016**, *51*, 6019-6034.
20. Bajpai, S. K.; Chand, N.; Ahuja, S.; Roy, M. K., Vapor induced phase inversion technique to prepare chitosan/microcrystalline cellulose composite films: synthesis, characterization and moisture absorption study. *Cellulose.* **2015**, *22*, 3825-3837.
21. Ghanbarzadeh, B.; Almasi, H.; Entezami, A. A., Improving the barrier and mechanical properties of corn starch-based edible films: Effect of citric acid and carboxymethyl cellulose. *Ind. Crop. Prod.* **2011**, *33*, 229-235.
22. Wang, Z.; Sun, X.-x.; Lian, Z.-x.; Wang, X.-x.; Zhou, J.; Ma, Z.-s., The effects of ultrasonic/microwave assisted treatment on the properties of soy protein isolate/microcrystalline wheat-bran cellulose film. *J. Food. Eng.* **2013**, *114*, 183-191.
23. González, A.; Strumia, M. C.; Alvarez Igarzabal, C. I., Cross-linked soy protein as material for biodegradable films: Synthesis, characterization and biodegradation. *J. Food. Eng.* **2011**, *106*, 331-338.
24. Xie, D.-Y.; Song, F.; Zhang, M.; Wang, X.-L.; Wang, Y.-Z., Roles of Soft Segment Length in Structure and Property of Soy Protein Isolate/Waterborne Polyurethane Blend Films. *Ind Eng Chem. Res.* **2016**, *55*, 1229-1235.
25. Li, Y.; Chen, H.; Dong, Y.; Li, K.; Li, L.; Li, J., Carbon nanoparticles/soy protein isolate bio-films with excellent mechanical and water barrier properties. *Ind. Crop. Prod.* **2016**, *82*, 133-140.
26. Koshy, R. R.; Mary, S. K.; Thomas, S.; Pothan, L. A., Environment friendly green composites based on soy protein isolate – A review. *Food Hydrocolloid.* **2015**, *50*, 174-192.
27. Wang, X.; Hu, L.; Li, C.; Gan, L.; He, M.; He, X.; Tian, W.; Li, M.; Xu, L.; Li, Y.; Chen, Y., Improvement in physical and biological properties of chitosan/soy protein films by surface grafted heparin. *Int. J. Biol. Macromol.* **2016**, *83*, 19-29.
28. Li, C.; Luo, J.; Qin, Z.; Chen, H.; Gao, Q.; Li, J., Mechanical and thermal properties of microcrystalline cellulose-reinforced soy protein isolate–gelatin eco-friendly films. *RSC Adv.* **2015**, *5*, 56518-56525.
29. Carpiné, D.; Dagostin, J. L. A.; de Andrade, E. F.; Bertan, L. C.; Mafra, M. R., Effect of the natural surfactant Yucca schidigera extract on the properties of biodegradable emulsified films produced from soy protein isolate and coconut oil. *Ind. Crop. Prod.* **2016**, *83*, 364-371.
30. Pang, J.; Wu, M.; Zhang, Q.; Tan, X.; Xu, F.; Zhang, X.; Sun, R., Comparison of physical properties of regenerated cellulose films fabricated with different cellulose feedstocks in ionic liquid. *Carbohyd. Polym.* **2015**, *121*, 71-8.
31. Yu, H.; Yan, C.; Lei, X.; Qin, Z.; Yao, J., Novel approach to extract thermally stable cellulose nanospheres with high yield. *Mater. Lett.* **2014**, *131*, 12-15.
32. Ghaderi, M.; Mousavi, M.; Yousefi, H.; Labbafi, M., All-cellulose nanocomposite film made from bagasse cellulose nanofibers for food packaging application. *Carbohyd. Polym.* **2014**, *104*, 59-65.
33. Xu, F.; Zhang,W.; Zhang, S.; Li, L.; Li, J.; Zhang, Y. Preparation and characterization of poly(vinyl alcohol) and 1,2,3-propanetriol diglycidyl ether incorporated soy protein isolate-based films. *J. Appl. Polym. Sci.* **2015**, 132.
34. Jensen, A.; Lim, L. T.; Barbut, S.; Marcone, M., Development and characterization of soy protein films incorporated with cellulose fibers using a hot surface casting technique. *Lwt-Food Sci. Technol.* **2015**, *60*, 162-170.
35. Lee, J.-A.; Yoon, M.-J.; Lee, E.-S.; Lim, D.-Y.; Kim, K.-Y., Preparation and characterization of cellulose nanofibers (CNFs) from microcrystalline cellulose (MCC) and CNF/polyamide 6 composites. *Macromol. Res.* **2014**, *22*, 738-745.
36. Yu, L.; Zhang, Y.; Zhang, B.; Liu, J., Enhanced antibacterial activity of silver nanoparticles/halloysite nanotubes/graphene nanocomposites with sandwich-like structure. *Sci. Rep.* **2014**, *4*, 4551.

37. Lee, J.-H.; Yang, H.-J.; Lee, K.-Y.; Song, K. B., Physical properties and application of a red pepper seed meal protein composite film containing oregano oil. *Food Hydrocolloid.* **2016**, *55*, 136-143.
38. Zhang, W.; Chen, J.; Chen, Y.; Xia, W.; Xiong, Y. L.; Wang, H., Enhanced physicochemical properties of chitosan/whey protein isolate composite film by sodium laurate-modified TiO_2 nanoparticles. *Carbohyd. Polym.* **2016**, *138*, 59-65.
39. Kumar, R.; Anandjiwala, R. D.; Kumar, A., Thermal and mechanical properties of mandelic acid-incorporated soy protein films. *J. Therm. Anal. Calorim.* **2015**, *123*, 1273-1279.
40. Xiong, R.; Zhang, X.; Tian, D.; Zhou, Z.; Lu, C., Comparing microcrystalline with spherical nanocrystalline cellulose from waste cotton fabrics. *Cellulose.* **2012**, *19*, 1189-1198.
41. Song, X.; Zhou, C.; Fu, F.; Chen, Z.; Wu, Q., Effect of high-pressure homogenization on particle size and film properties of soy protein isolate. *Ind. Crop. Prod.* **2013**, *43*, 538-544.
42. Zhang, S.; Xia, C.; Dong, Y.; Yan, Y.; Li, J.; Shi, S. Q.; Cai, L., Soy protein isolate-based films reinforced by surface modified cellulose nanocrystal. *Ind. Crop. Prod.* **2016**, *80*, 207-213.
43. Galus, S.; Kadzińska, J., Whey protein edible films modified with almond and walnut oils. *Food Hydrocolloid.* **2016**, *52*, 78-86.
44. González, A.; Alvarez Igarzabal, C. I., Nanocrystal-reinforced soy protein films and their application as active packaging. *Food Hydrocolloid.* **2015**, *43*, 777-784.
45. Sharma, L.; Singh, C., Composite film developed from the blends of sesame protein isolate and gum rosin and their properties thereof. *Polym. Composite.* **2016**.
46. Kang, H.; Wang, Z.; Zhang, W.; Li, J.; Zhang, S., Physico-chemical properties improvement of soy protein isolate films through caffeic acid incorporation and tri-functional aziridine hybridization. *Food Hydrocolloid.* **2016**, *61*, 923-932.